



## ENERGETICAL AND OPERATIONAL CONSIDERATIONS AT DIRECT CURRENT MOTORS ASSOCIATED WITH STATIC CONVERTERS

Ion VLAD, Aurel CAMPEANU, Sorin ENACHE, Gabriela PETROPOL

University of Craiova, Romania, ivlad@em.ucv.ro

**Abstract** – All over of the deformed regime, the essential problem is to analyze the wave of voltage, current and power, associated to electromechanical equipment, to distinguish the most important harmonics and the most known analysis factors. Starting with this considerations, results the necessity to study the typical problems of the direct current motors associated with static converters, with the aim to obtain some indications about their optimal design, construction and operation.

**Keywords:** deformed regime, direct current motors, static converters.

### 1. INTRODUNCTION

The aim of this paper is to establish an algorithm which is the base of a program to study the drives with DC motors associated with static's converters, through presenting concrete examples. For calculus and a correct representation of the characteristics of starting and operating, is imposed a detailed analyze of the whole system machine – converter. In this way it could be made a quantification the effects of the deformed regime: the increase of the energies losses cost in use, reported to the standard regime, caused by the increase of active, reactive and deformed power. All this effects are depended on the quality of the materials used in the construction of the machine and converter, and so, could be established the optimal values of the electro mechanical solicitations.

### 2. ESTABLISHING THE MATHEMATICAL MODEL

It is considered that in the majority of electric drive, the current in load of the rectifier is continuous (regime assured by the smooth coil with great inductances serried with the Indus). The theoretical graphical representation shows a sensible reducing of the area of the broken current or, at the great load, even at their canceled, with known favorable consequences.

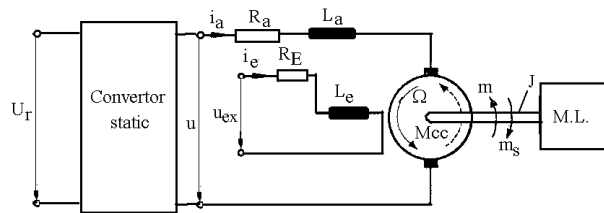


Figure 1: Electrical schema of the D.C. motor associated with static converter.

### 2.1. D.C. Motor feed by a Static Converter Commanded in Double Alternation

Using the known numerical methods [7], for the voltages of feed obtained from the rectifier, are finding the coefficients of the harmonically series,  $A_0$ ,  $M_k$ ,  $N_k$ , respective

$$U_0 = A_0, \quad U_k = \sqrt{\frac{M_k^2 + N_k^2}{2}}, \quad \alpha_k = \text{actg} \frac{M_k}{N_k} \quad (1)$$

and for supply voltage could be obtain the relation:

$$u = U_0 + \sum_{k=1}^{\infty} \sqrt{2} U_k \sin(k\omega t + \alpha_k) \quad (2)$$

$U_0$  - continuous component of voltage of the command angle  $\alpha$ ;  $U_k$  - effective value of the harmonic k of the voltage of the command angle  $\alpha$ ;  $\omega = 2\pi f$  - pulsation of the supply voltage...

The equations which are described the operation of the motor (fig. 1) in this case, when all values are varying in time is:

$$U_0 + \sum_{k=1}^{N_k} \sqrt{2} U_k \sin(k\omega t + \alpha_k) = R_a i_a + L_a \frac{di_a}{dt} + k_e n \Phi$$

$$2\pi J \frac{dn}{dt} = k_m \Phi i_a - M_r \quad (3)$$

$n$  – motor's revolution;  $i_a$  -current through the rotor;  $k_e, k_m$  -coefficients;  $R_a, L_a$  - resistance and inductivity of the stator,  $J$  - inertial torque of the whole motor - load;  $M_r$  - resistant total torque.

To realized a stabilized regime, knowing the input quantities: voltage (continuous components and its harmonics) and the resistant torque  $M_r$  (constant or variable), it will be solve the system of differential equations (3), obtaining the solutions of system,  $i_a, n$  (current and speed), and then  $u_e, m$  (electromotive voltage and electromagnetically torque) as quantities of response. Total current, will have an important continuous component (that which equalized the resistant torque to ax) and superior harmonics:

$$i = I_0 + \sum_{k=1}^{N_k} \sqrt{2} I_k \sin(k\omega t + \alpha_k - \varphi_k) \quad (4)$$

similar, results the speed,

$$n = n_0 + \sum_{k=1}^{N_k} n_{mk} \sin(k\omega t + \beta_k) \quad (5)$$

but with a reduced number of harmonics, because the superior's harmonics of the current are establishing variables torques with the medium value approximate null and taken account by the important value of the inertial torque it will be observe that the speed of the motor is approximate constant.

## 2.2. Calculus Program

Starting with the non linear system equations (3), adapted for the case of a DC motor with separate excitation, using the knowing numerical calculation methods, it was realized a calculus program based on fourth Runge Kutta methods and it was founded the solutions of the system in stabilized regime.

This program allowed studying the operation of the motors when the supply voltage is varying (curve of time variation) and also the resistance and inductance introduced in the rotor circuit, total inertial moment or the resistant torque to the ax. For this study it taking away two cases: was starting with the ideal case, when the inducing flux remains constant with the load (is neglected the effect of demagnetization made by the transversal reaction of the inductor) and the second case was the real case when those quantities are variable with load because of the magnetic saturation.

The variation in time of the voltage, respective of the resistant torque is given matricidal or analytical, using the appropriate relations. All of this can induced big variations of the speed of the rotor, of the current from induce and of the torque. When we consider the reaction of the induced (for a complicated transient process), the system of equations is powerful non

linear and the program of calculus is very complicated and the time for calculus is very big.

This program can allow directing the results towards the aspect demanded by the designer or by the beneficiary.

## 2.3. Factors of Harmonical Analyses

On the side of the wavy current, these factors are: factor of peak, factor of shape and factor of wave,

$$k_v = \frac{M_m}{M} \quad k_f = \frac{M}{M_{med\ red}} \quad k_o = \frac{M_{max} - M_{min}}{2M_0} \cdot 100 \quad (6)$$

and on the side of the alternative current we have: factor of distortion, factor of deformation:

$$THD = \sqrt{\sum_{k=2}^{\infty} M_k^2} / \sqrt{\sum_{k=1}^{\infty} M_k^2} \quad (7)$$

## 3. SIMULATIONS AND EXPERIMENTAL RESULTS

The simulations were made using the calculus of the program shown in § 2.2 studying the behavior of a D.C. motor with separated excitation supplying by an order rectifier. Nominal data of the motor and the parameters are:  $P_N = 2,7$  kW;  $U_N = 220$  V;  $n_N = 1500$  rot/min.;  $I_N = 15$  A, and the parameters of the derivation motor are:  $U_{ex} = 220$  V;  $I_{ex} = 0,55$  A,  $R_{ad} = 1,702$   $\Omega$ ;  $L_{ad} = 23$  mH;  $J = 0,04$   $kgm^2$ ,  $k_e = 32,4$ ;  $k_m = 309,4$ ;  $\Phi_d = 0,00394$  Wb, respective at series DC motor:  $R_{as} = 2,27$   $\Omega$ ;  $L_{as} = 44,2$  mH;  $J = 0,04$   $kgm^2$ ,  $k_e = 20,8$ ;  $k_m = 198,6$ ;  $\Phi_s = 0,00377$  Wb.

The same motors were also used to made the experiments, and for the measurements was used the multifunctional device, the analyzer of harmonics Fluke 41B. Data transfer and the work with the computer are made with the soft Fluke View R41. With this device were measured the currents, the voltages and powers in alternative currents (on the side of the network, to the input of converter) and in wavy current (to the connecting terminals, to the output of the converter).

To make an efficient evaluation between the experimental determinations and those obtained by simulation, will be represented successively this results. For an easily interpretation of the results in all the graphical representations, the quantities are given in relative units. Related quantities are:  $P_N = 2,7$  kW for power,  $I_N = 15$  A for current,  $U_N = 220$  V for voltage,  $n_N = 1500$  r/m for speed.

To make correct simulations it taken account the dependence of the motor's inductances with the load factor  $k_s = I_a / I_{aN}$ . The calculus of this inductance was made according with the literature [3], [4], considering all the components of this inductance: induce inductance, field winding inductance, series winding inductance and auxiliary pole's inductance. In fig.2 we can see the way of varying of the inductances of this two motors (series and derivation  $L_{ad}, L_{as}$ ), reported to the load factor because of saturation of the magnetic circuit (the index  $\neq ct.$ ,  $=ct.$  shows us the consideration of the magnetic saturation, respectively it's neglected).

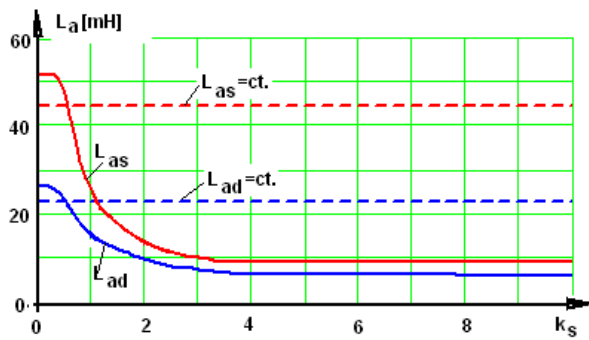


Figure 2: Inductances versus load factor  $k_s$  at derivation motor (blue curves), and series motor (red curves), for saturated machine (continuous line), respectively no saturated (dots line).

At the derivation motor, in the rated point, the obtained value is much closed with that measured experimental, ( $L_{ad} = 23$  mH versus  $L_{ad\ exp} = 22,1$  mH), and for the series motor was obtain ( $L_{as} = 44,2$  mH versus  $L_{as\ exp} = 43,7$  mH).

At the analysis of the dynamic regimes for simplicities we consider the machine's flux constant. So, the method used to simulate the dynamical regime is much simplified, without specify the deviation from the real case.

When we made definite pre-determinations on the dynamic characteristics (like in the case of the DC motor feed by static's converters), it is imposed to consider the demagnetization effect of the induce reaction on the magnetic champ of inductor, because the current in machine has important oscillations. For the derivation motor, are shown in fig. 2 the curves of magnetic flux  $\Phi_{d\ nes}, \Phi_{d\ sat}$  (calculate for the case when is neglected or is taken in consideration the reaction of induce), reported to the load of machine.

We can see a marked decrease (about 30%) of the flux at big load, followed with a constant value because of the magnetic saturation (the effects of magnetization

and demagnetization are equalized in the saturated zone).

At the rated load, the decrease of the used flux is 8%, the factor of magnetic saturation is  $k_s = 1,6$ .

At the series motor, the excitation's turn ampere is dependent with the load current. The operating point takes different positions on the magnetization characteristic. So, the reaction field of the induce demagnetization very little the machine in the areas of flexion of the characteristic (fig. 3). So the magnetic flux  $\Phi_{s\ nes}, \Phi_{s\ sat}$  (calculated without respective with the influence of the saturation), could be considered equal.

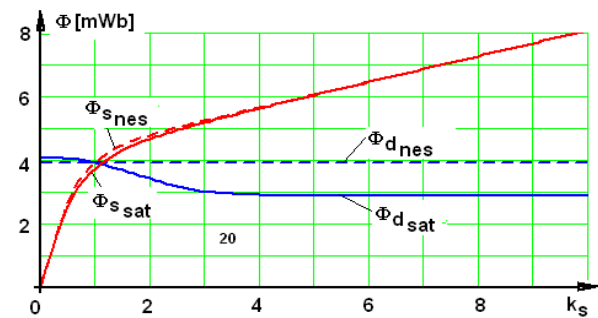


Figure 3: Useful flux versus load factor  $k_s$  at the derivation motor (curves with blue), and at the series motor (curves with red), for saturated machine (continuous line), respectively no saturated (dots line).

### 3.1. D.C. Motor Suplies from a Rectifier in non Order Bridge Operating in Load

#### 3.1.1. Harmonically Analyses of the Quantities Reported on the Network

The aim of the experiments was to measure the voltage, the current, and the factors of the harmonic analyses and to establish the curves of time variation and the harmonically analysis of these quantities. In following figures are shown the recorded curves to the input of the rectifier (on the side of supply network), for the unload operation of the motor (fig. 4 –voltage and fig. 5 – current), and also the harmonically spectrum.

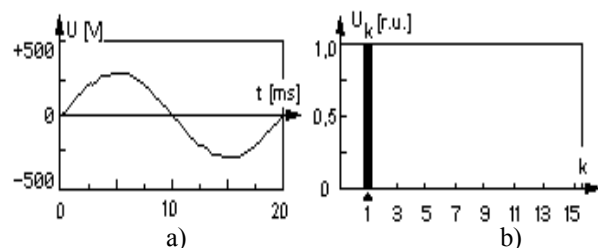


Fig. 4. Recording curve for the voltage of the network (fig. a), and it's harmonically spectrum (fig.b).

For the same regime of operation and the same supply voltage (fig. 4), curves obtained through the simulation for current is shown in figure 6.

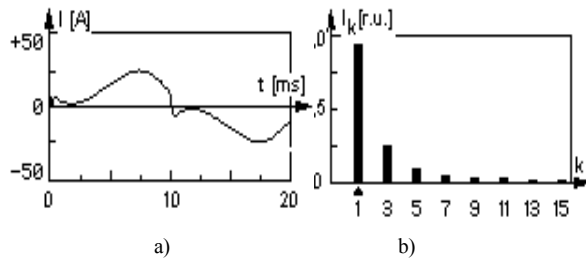


Figure 5: Recording curve for the current of the network (fig. a), and its harmonically spectrum (fig.b).

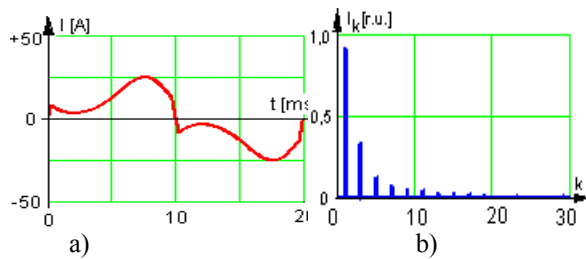


Figure 6: Simulation curve for the current of the network (fig. a), and its harmonically spectrum (fig.b).

Quantitative difference in dynamic regime between the real curves and the classical appear because of the magnetic saturation which modified essential the inductance of the machine (fig. 2) and the useful flux (fig. 3). For the regime analyzed in figure 7 we have:  $i_a$  - current curve (with red and continuous line) for the real regime with saturation;  $i_{a\ nes}$  - current curve obtain in a classical way (blue, thin line);  $i_{a\ exp}$  - current curve established experimental (with black dots line). For exactly determinations, taken in consideration the saturation is obligatory, resulting curves almost overlap for the currents and a square average deviation very small:

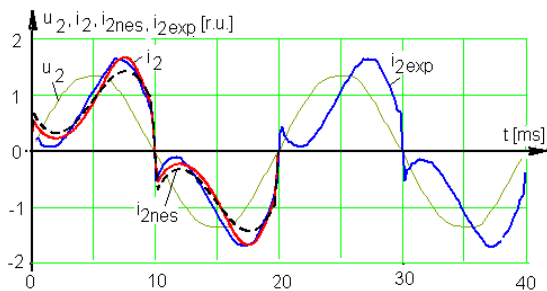


Figure 7: Simulation curves and real curves in per unit for the current at the load operation:  $i_2$  -real curve of the network current;  $i_{2\ nes}$  - classical curves;  $i_{2\ exp}$  -testing curve.

$$\varepsilon_{Ia} = \sqrt{\frac{1}{T} \sum_{j=1}^n (i_{2j} - i_{2\ exp j})^2 \cdot t_j} = 6,9\% \quad (8)$$

### 3.1.2. Harmonical Analyze of the Quantities Reported on the Motor

Following, also for the load operation, are presented the values measured and the curves recorded, reported on motor, for the output of the rectifier, (fig. 8 – voltage and fig. 9 –current), accompanied with the harmonics spectrums.

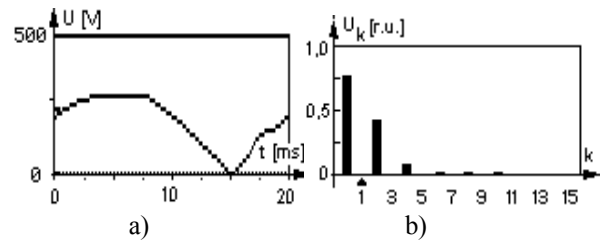


Figure 8: Recording curve of the voltage (fig. a), and its harmonically spectrum (fig.b).

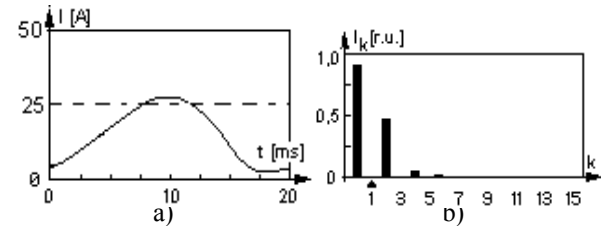


Figure 9: Recording curve of the current (fig. a), and its harmonically spectrum (fig.b).

Using the simulation for the same regime was obtained the curve of voltage (fig. 10) and the curve of current (fig. 11).

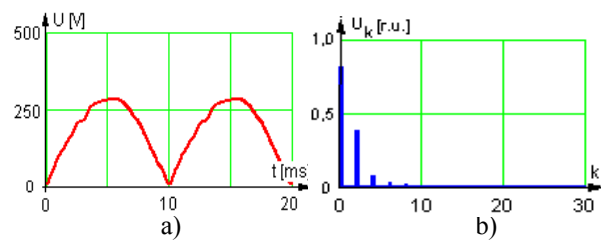
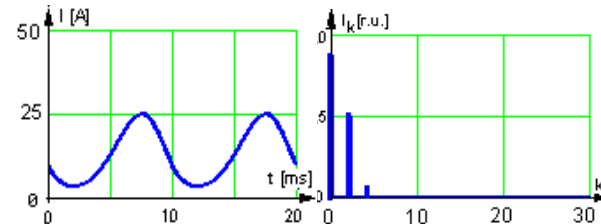


Figure 10: Simulation curve of the voltage (fig. a), and its harmonically spectrum (fig.b).

There are quantitative differences in dynamic regime between the real curves and the classical curves because of the magnetic saturation.



a) b)  
Figure 11: Simulation curve of the current (fig. a), and its harmonically spectrum (fig.b).

In figure 12 was kept the mode of abbreviation and representation, red color for the real regime  $i_a$ , blue color for the classical regime  $i_{anes}$  and black for the test curve  $i_{aexp}$ . At the consideration of the magnetically saturation results curves almost overlap for the currents and a square average deviation very small:

$$\varepsilon_{Ia} = \sqrt{\frac{1}{T} \sum_{j=1}^n (i_{aj} - i_{aexpj})^2 \cdot t_j} = 4,8\% \quad (9)$$

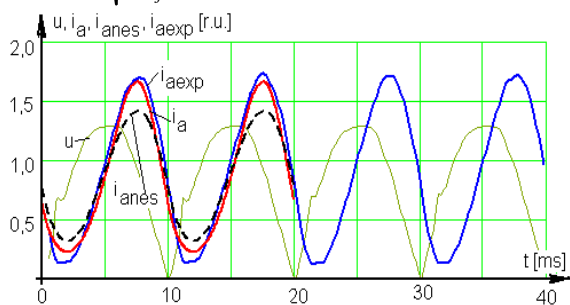


Figure 12: Simulation and testing current's curves in per unit for the operation in load of the motor with excitation in derivation:  $i_a$  -real curve of current;  $i_{anes}$  -classical curve;  $i_{aexp}$  - test curves.

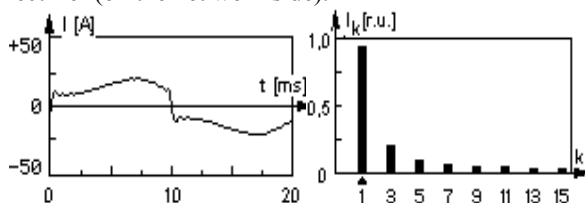
In table no.1 are the calculated values and the measured one, for the DC motor with excitation in derivation on the net side and also on the motor side. The numerical calculus and tests taken account: voltage, current, power, harmonically analyzing factors. The errors are calculated with:

$$\varepsilon_j (\%) = 100 \left| \frac{I - I_{exp}}{I_{exp}} \right| \quad (10)$$

### 3.2. Series D.C. Motor Supplies from a Monophased Rectifier in Bridge Operating in Load

#### 3.2.1. Harmonically Analyses of the Quantities Reported on the Network

The aim of the tests with the D.C. series motor was to find the voltage, the current, the power, their time variation curves and harmonically analyses of those quantities. For the same voltage supplies (fig.4), resulted the current curve (fig.13) recorded at the input of the rectifier (on the net work side).



a) b)  
Figure 13: Recording current curve on the net work side (fig. a) and its' harmonically spectrum (fig.b).

Keeping the operating regime and the voltage supplies was obtained by simulation curve fig. 14 for the current.

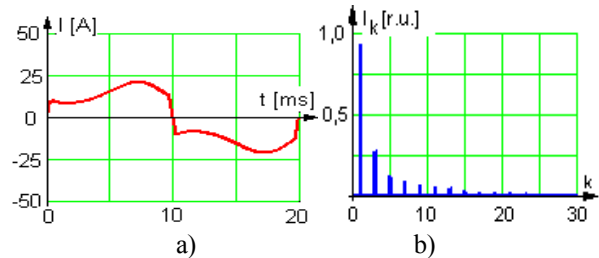


Figure 14: Current curve obtain by simulation (fig. a), and its' harmonically spectrum (fig.b).

Also in fig. 14 could be seen the quantitative difference in dynamic regime between the classic curves and the dynamics curves, determinates by the magnetically saturation which modify in large the inductance of the machine (fig. 2) and also the useful magnetic flux (fig. 3). For the analyzed regime in figure 15 we have:  $i_2$  - current curve (with red and continuous line) for the real regime with the saturation;  $i_{2nes}$  - current curve obtain in classic way (with black dots line);  $i_{2exp}$  - current curve obtain by tests (with blue line). Taking account the saturation are obtain curves almost overlap for the currents and a square average deviation very small:

$$\varepsilon_{Ia} = \sqrt{\frac{1}{T} \sum_{j=1}^n (i_{2j} - i_{2expj})^2 \cdot t_j} = 5,6\% \quad (11)$$

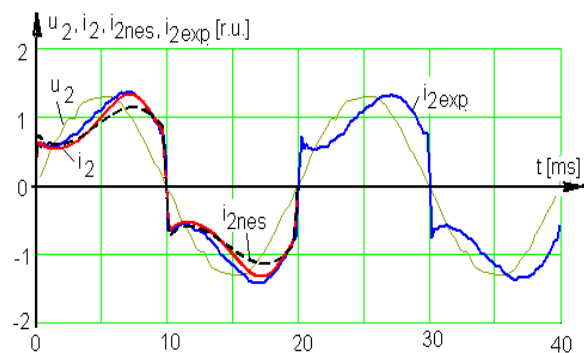


Figure 15: Currents curves in per unit obtained by simulation and by tests under load operation:  $i_2$  - real curve of the network current;  $i_{2nes}$  -classical curves of the currents;  $i_{2exp}$  - curve obtain by test.

### 3.2.2. Harmonically Analyses of the Quantities Reported on the Motor Side

Following are shown for the load operation the measured values and the recording curves on the motor side, at the output of the rectifier (fig. 16 – voltage and fig. 17 – current), with their harmonically specters.

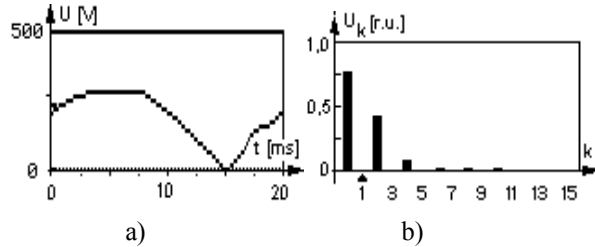


Figure 16: Recording curve of voltage (fig. a), and its' harmonically spectrum (fig.b).

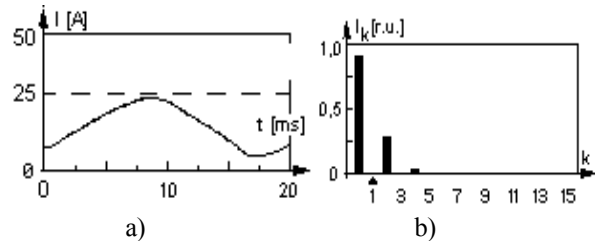


Figure 17: Recording curve of current (fig. a), and its' harmonically spectrum (fig.b).

For the same regime was obtain the voltage curve (fig. 18), and the current curve (fig. 19).

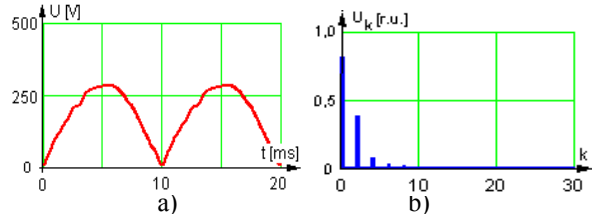


Figure 18: Voltage curve obtained by simulation (fig. a), and its' harmonically spectrum (fig.b).

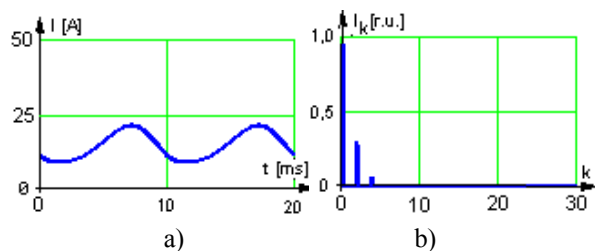


Figure 19: Current curve obtained by simulation (fig. a), and its' harmonically spectrum (fig.b).

It could be seen the quantitative difference in dynamic regime between the real curves and the classical curves (fig.20), the symbols being those known in literature. Overlapping the currents curves (by tests and simulation) is justified by the very small square average deviation:

$$\varepsilon_{I_a} = \sqrt{\frac{1}{T} \sum_{j=1}^n (i_{a_j} - i_{a_{exp_j}})^2 \cdot t_j} = 2,4\% \quad (12)$$

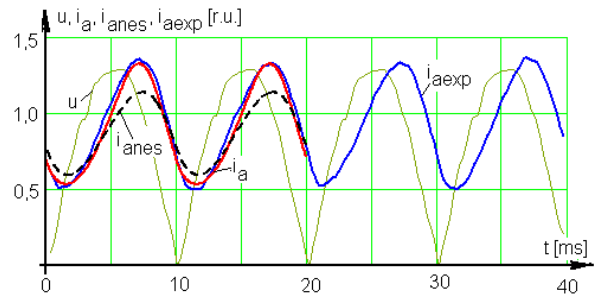


Figure 20: Series D.C. motor currents curve in per unit at load operation:  $i_a$  - real current curve;  $i_{anes}$  - classical current curve;  $i_{aexp}$  - curve finding by tests.

In table no.2 are shown the calculated values and the measured ones, at the series D.C. motor on the network side and on the motor side. Numerical calculus and the tests taken account with: voltage, current, powers and factors of harmonically analyses. The errors are calculated with (10).

Table no. 1

Calculated and measured quantities of the derivation motor loaded with rated load							
Network side				Motor side			
Quantities	Calc.	Meas.	Error	Quantities	Calc.	Meas.	Error
$U$ (V)	206	205	0,4%	$U$ (V)	202,9	202	0,4%
$U_1$ (V)	205	204	0,4%	$U_0$ (V)	183,5	181	1,3%
$k_{vU}$	1,29	1,27	1,7%	$k_{vU}$	1,28	1,29	0,7%
$THD_U$ (%)	2,95	2,7	8,6%	$k_{oU}$ (%)	69,3	67,8	2,2%
$I$ (A)	16,7	16,2	3,1%	$I$ (A)	16,85	16,4	2,7%
$I_1$ (A)	15,2	14,9	2,0%	$I_0$ (A)	14,66	14,2	3,3%
$k_{vI}$	1,67	1,69	1,2%	$k_{vI}$	1,85	1,83	1,1%
$THD_I$ (%)	41,3	37,5	9,2%	$k_{oI}$ (%)	89,2	84,3	5,6%
$S$ (VA)	3672	3500	4,9%	$S$ (VA)	3661	3510	4,3%
$P$ (W)	2930	2790	4,7%	$P$ (W)	2922	2890	1,1%
$Q$ (VAR)	1613	1600	0,8%	$Q$ (VAR)	1607	1580	1,7%
$D$ (VAD)	1517	1365	9,8%	$D$ (VAD)	1504	1209	19%
$\cos \varphi$	0,798	0,83	3,8%				
$\cos \varphi_1$	0,876	0,86	1,8%				

With the predetermined quantities could be calculated the real efficiency of the motor (considering all the losses), the useful mechanical power at the shaft, mechanical torque, etc., and those values could be compared with those known by the classical operation (in continuous

current).

To establish the efficiency of the D.C. drives supplied by static's converters could be calculated the supplementary expenses in use, on a known period of time, with the relation:

$$C_{exp} = C_{el} T_{ri} N_{ore} \Sigma p_0 = \dots \quad (13)$$

where:  $C_{el} = 3,22$  lei/kWh is the cost of one kWh;  $T_{ri} = 6$  years – time to recuperate the investment;  $N_{ore} = 3545$  hours – numbers of hours of operating in an year;  $\Sigma p_0 = \Sigma p_{ond} - \Sigma p = 443$  W - total supplementary losses in the machine caused by the operation in rippled current.

#### 4. CONCLUSIONS

The curves of the variation in time of all predetermined quantities are very close as shape, with those recorded. The validity of the predetermination methods proposed in this paper for the two types of motors (series and derivation) is justified by the errors small less by 5%, between the values of calculated and measured quantities. The processed results show:

- it could be established the factor of power of the drive system, the distortion factor of the absorbed current, the content of harmonics, and also a strategies to improve the unfavorable effects;
- quantitative differences in dynamic regime between the real curves and the classical curves appeared because of the magnetic saturation which modifies the inductance of the machine and useful flux.

Table no.2

Calculated and measured quantities of the series motor loaded with rated load							
Network side				Motor side			
Quantities	Calc.	Meas.	Error	Quantities	Calc.	Meas.	Error
$U$ (V)	206	205	0,4%	$U$ (V)	202,9	202	0,4%
$U_1$ (V)	205	204	0,4%	$U_0$ (V)	183,5	181	1,3%
$k_{vU}$	1,29	1,27	1,7%	$k_{vU}$	1,28	1,29	0,7%

$THD_U$ (%)	2,95	2,7	8,6%	$k_{oU}$ (%)	69,3	67,8	2,2%
$I$ (A)	14,8	15	1,3%	$I$ (A)	14,83	14,3	3,5%
$I_1$ (A)	13,9	14,3	2,7%	$I_0$ (A)	14,25	13,8	3,2%
$k_{vI}$	1,42	1,38	2,8%	$k_{vI}$	1,39	1,38	0,8%
$THD_I$ (%)	33,1	32,5	1,8%	$k_{oI}$ (%)	43,7	41,5	5,1%
$S$ (VA)	3253	3100	4,9%	$S$ (VA)	3243	3130	4,4%
$P$ (W)	2962	2900	2,1%	$P$ (W)	2951	2920	1,1%
$Q$ (VAR)	805	780	3,2%	$Q$ (VAR)	812	860	5,8%
$D$ (VAD)	1077	748	29,2%	$D$ (VAD)	1065	632	38%
$\cos \varphi$	0,915	0,91	0,5%				
$\cos \varphi_1$	0,935	0,93	5,3%				

#### References

- [1] M. Ancau, L. Nistor: *Tehnici numerice de optimizare în proiectarea asistată de calculator*. Bucuresti, Editura Tehnică, 1996.
- [2] G. Andronescu: *Simularea numerică a acționărilor electrice cu mașini de curent continuu*. Editura Politehnică București, 2000.
- [3] M. Biriescu, V. Cretu, M. Mot: *Testing of Electrical Machines Using a Data Acquisition and Processing System*. Workshop on Electrical Machines' Parameters. Cluj Napoca, Romania, 2001.
- [4] A. Campeanu: *Introducere în dinamica mașinilor electrice de curent alternativ*. București, Editura Academiei Române, 1998.
- [5] I. Daniel, I. Munteanu: *Metode numerice în ingineria electrica*. Bucuresti, Editura Matrix Rom, 1998.
- [6] T. Dordea: *Metoda IPT de calcul cu ordinatorul electronic al masinilor electrice de inductie*. Programul IND, IP Timisoara, 1994.
- [7] M. Ghinea, V. Firețeanu: *Matlab –Calcul umeric.Grafică. Aplicații*. București, Editura Teora, 1999.
- [8] I. Vlad, S. Enache, G. Petropol: *Energetic Aspects About the Operation of the Engines of D.C. Feeds by the Static Converters*. Cluj-Napoca, Acta Electrotehnica, Vol. 44, No. 3, 2004, p.107-111.